



NASA SPACE RADIATION PROGRAM

Shifting Focus from Macroscopic to Microscopic and Nanoscopic Simulations of Tracks and Therapeutic Dose

Ianik Plante

Wyle Science, Technology and Engineering
1290 Hercules, Houston, TX 77058

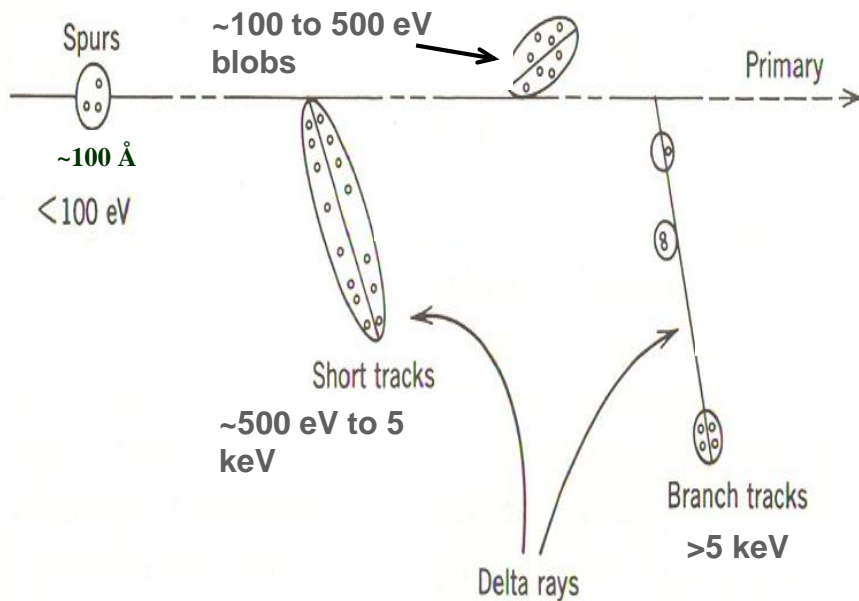
International Symposium on Ion Therapy
October 15-16, 2015

Radiation Track Structure



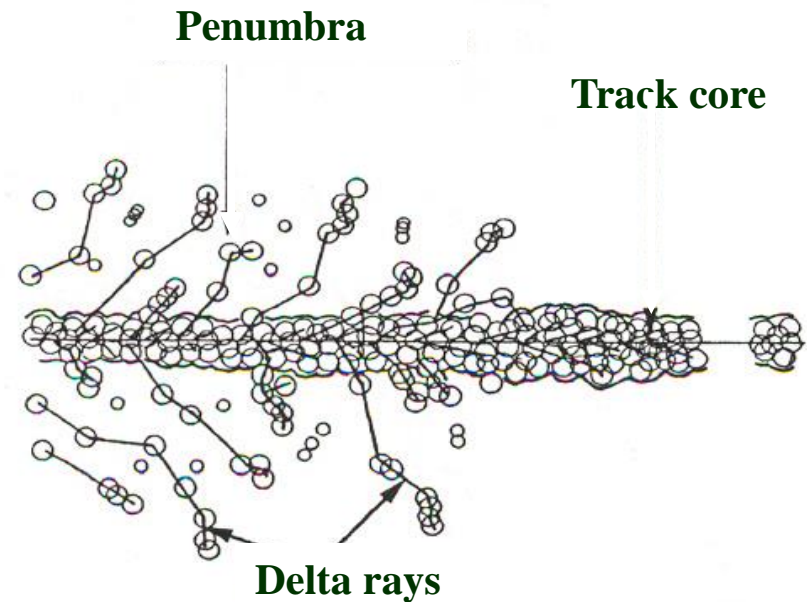
- ❑ The energy deposition by heavy ions is highly heterogeneous and dependent on the type and energy of the ion
- ❑ The interaction leads to the formation of radiolytic species such as $\text{H}\cdot$, $\cdot\text{OH}$, H_2 , H_2O_2 , e^-_{aq} , ...

Primary energy loss events in low-LET tracks



Mozumder A, Magee JL. Radiat Res 1966; 28:203

Primary energy loss events in high-LET tracks

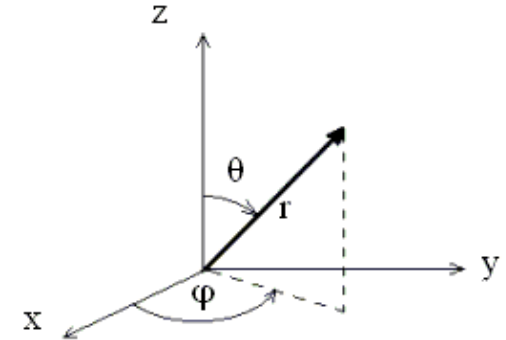


Ferradini C. J Chem Phys 1979; 76:636

□ Particles

- Position (x,y,z)
- Energy (E)
- Direction (θ, φ)

$$\vec{v} = \begin{bmatrix} \sin(\theta) \cos(\varphi) \\ \sin(\theta) \sin(\varphi) \\ \cos(\theta) \end{bmatrix}$$



□ Cross sections

- Probability of interaction between radiation and matter

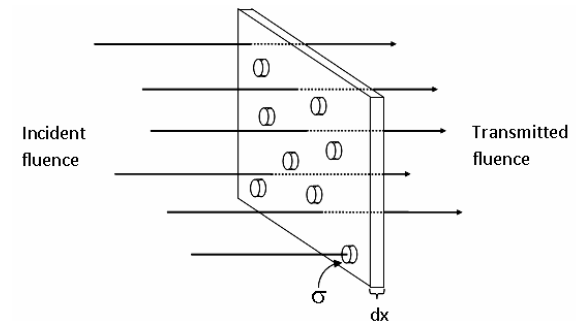
$$dI = -I n \sigma dx$$

I: Incident fluence

n: Density of targets

dx: Width

σ : Cross section

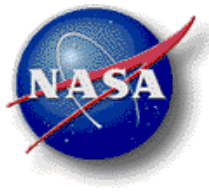


- **Cross sections** (units: cm²)
- Mean free path λ (units: cm)

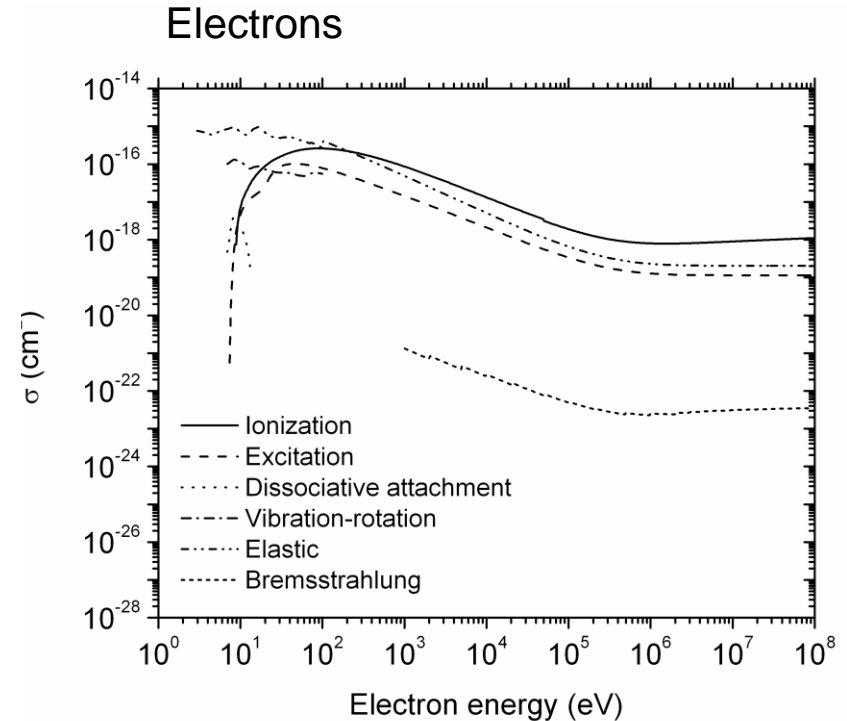
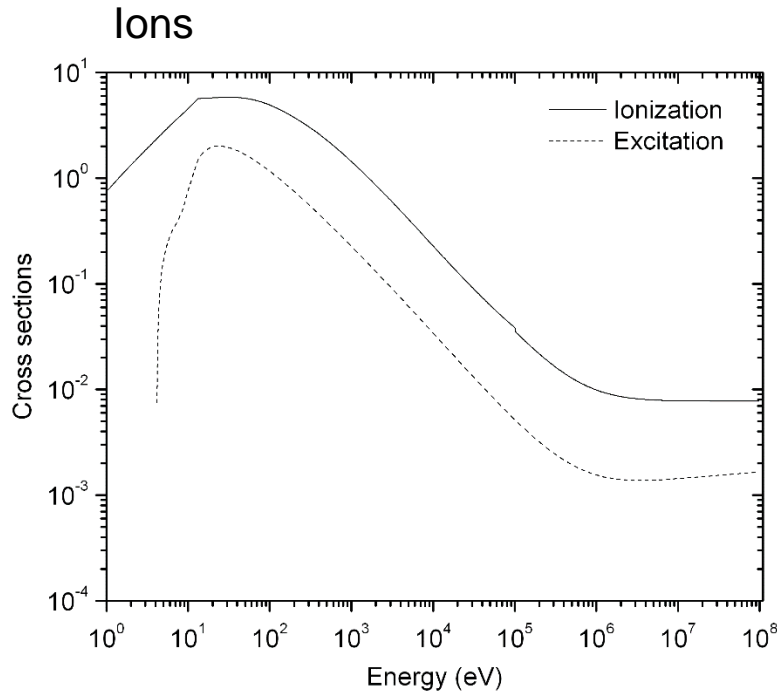
$$I(x) = I(0) \exp(-x / \lambda(E))$$

$$\lambda(E) = 1 / (N \sigma(E))$$

Particles Transport Basics



□ Cross sections used in RITRACKS



The cross sections for ions are scaled with Z_{eff} :

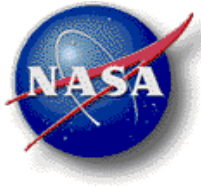
$$\frac{d\sigma_{\text{ion}}(v)}{dW} = Z_{\text{eff}}^2 \frac{d\sigma_{\text{proton}}(v)}{dW}$$

$$Z_{\text{eff}} / Z = 1 - \exp(-125\beta^2 / Z^{2/3})$$

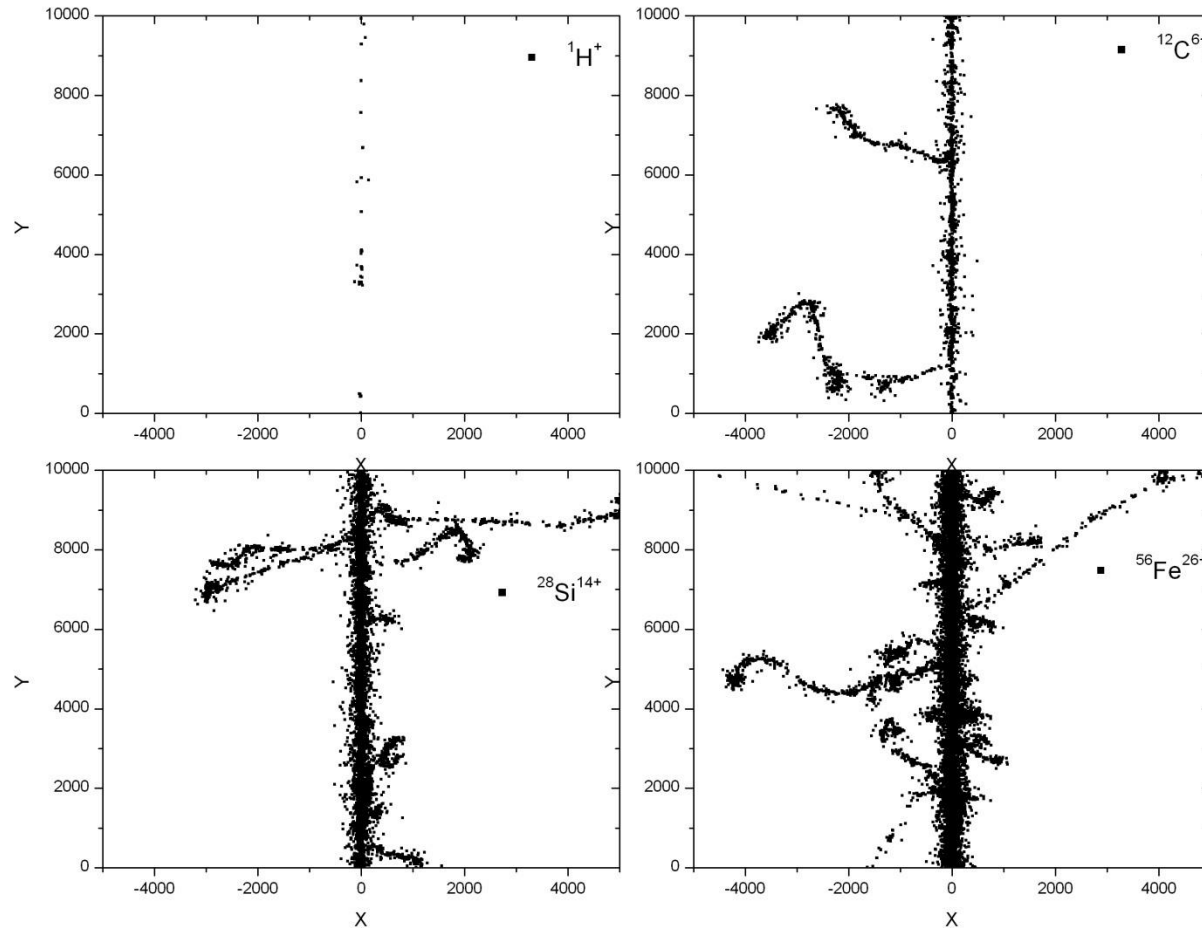
v : velocity of the ion

β : relativistic v/c

Radiation Track Structure



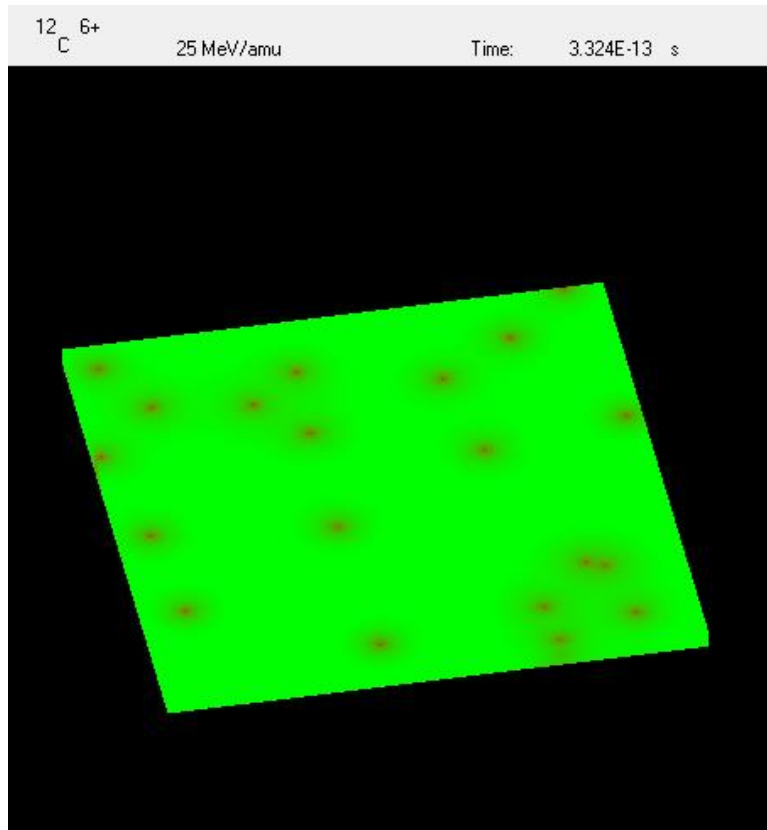
Simulation of $^1\text{H}^+$, $^{12}\text{C}^{6+}$, $^{28}\text{Si}^{14+}$ and $^{56}\text{Fe}^{26+}$ tracks, 100 MeV/amu



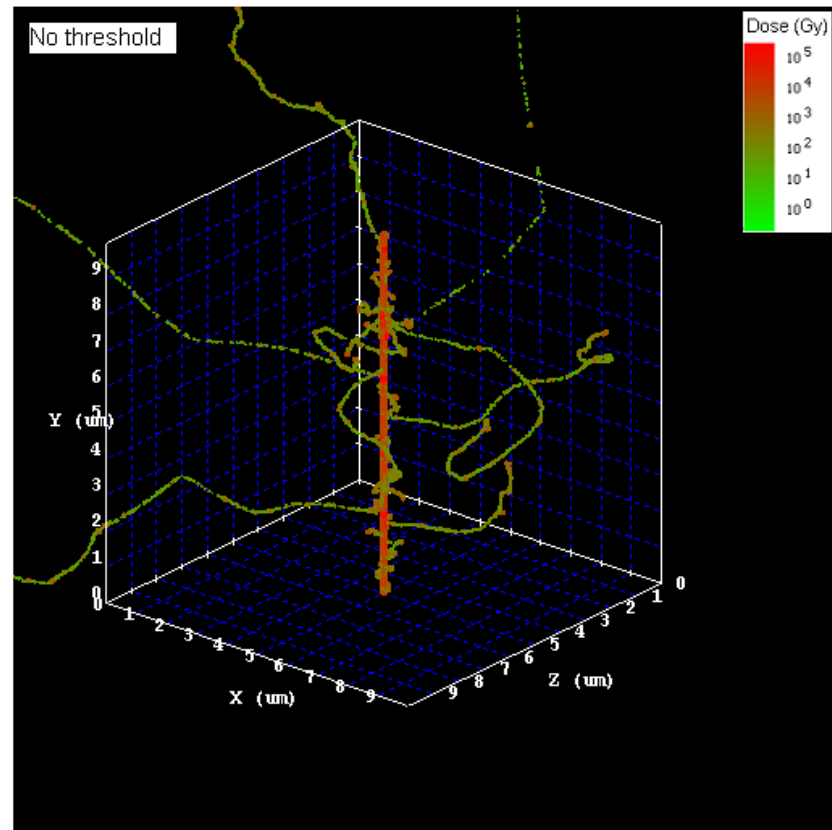
Voxel Dosimetry



Amorphous tracks



Stochastic tracks



1 GeV/amu $^{56}\text{Fe}^{26+}$ ion

LET~150 keV/ μm

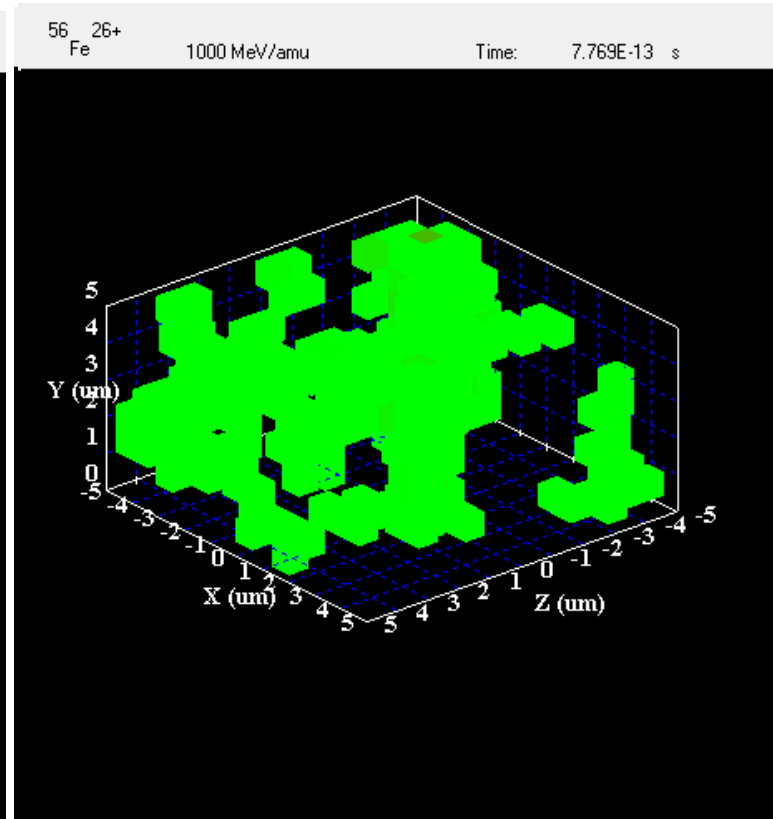
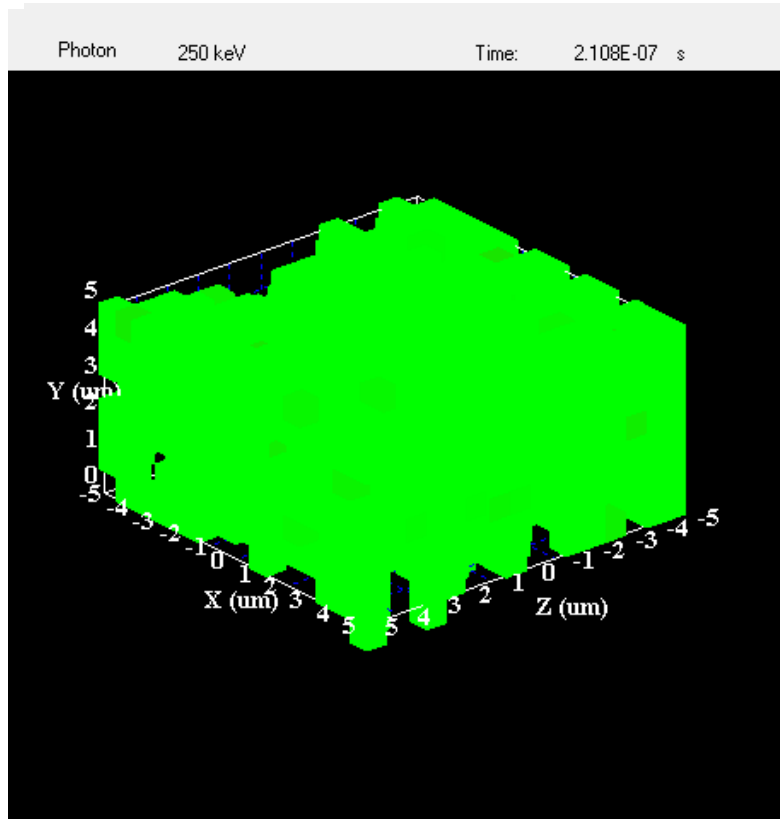
Voxels: 40 nm \times 40 nm \times 40 nm

Voxel Dosimetry

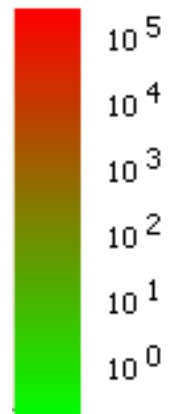


Photons 250 keV

Iron 1000 MeV/u



Dose (Gy)



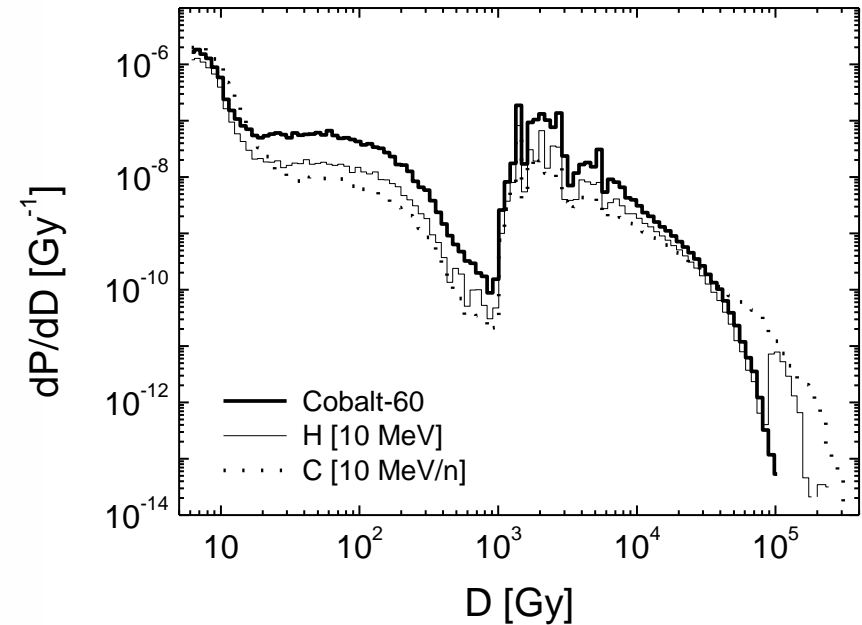
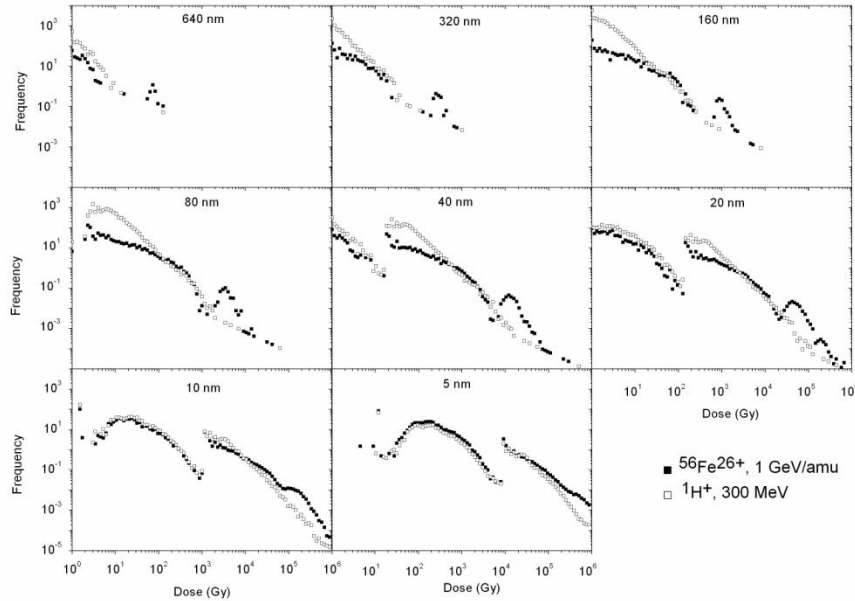
Voxels size: 640 nm

Dose to irradiated volume is 0.22 Gy in both cases

More on Voxel Dosimetry

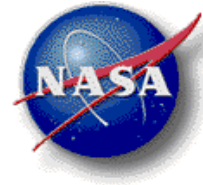


❑ This was presented at the RRS meeting 2010...



Found similar results in this paper:

Beuve, M. et al. *Nucl. Instr. Meth. Phys. Res. B* **267**, 983-988 (2009).



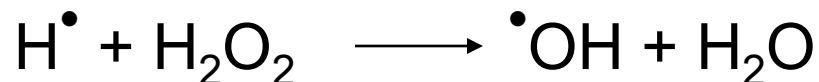
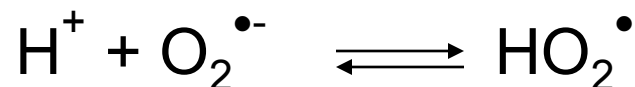
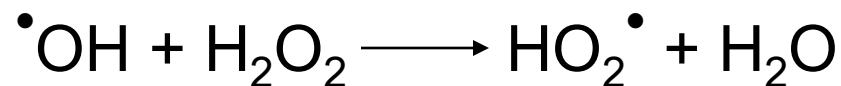
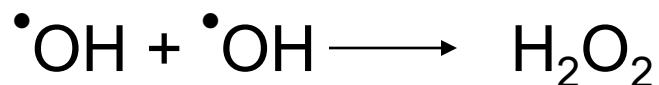
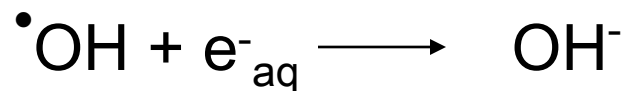
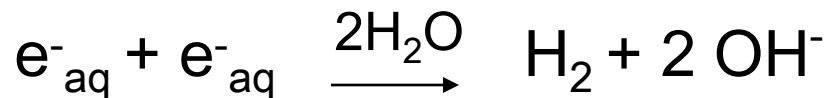
□ $\sim 10^{-12} - 10^{-6} \text{ s}$

- Particles diffusion
- Chemical reactions

$$G(X) = \frac{\text{Number of chemical species created}}{100 \text{ eV deposited energy}}$$

- The radiolytic species are not uniformly distributed, so conventional chemical kinetics models cannot be used.
- An approach based on Green's functions of the diffusion equation (DE) is used.

Examples of chemical reactions:





□ Partially diffusion-controlled reaction with rate k_a and reaction radius R



$$4\pi R^2 D \left. \frac{\partial p(r, t | r_0)}{\partial r} \right|_{r=R} = k_a p(R, t | r_0) \quad (\text{Boundary condition})$$

$$4\pi r_0 p(r, t | r_0) = \frac{1}{\sqrt{4\pi Dt}} \left\{ \exp\left[-\frac{(r - r_0)^2}{4Dt}\right] + \exp\left[-\frac{(r + r_0 - 2R)^2}{4Dt}\right] \right\} + \alpha W\left(\frac{r + r_0 - 2R}{\sqrt{4Dt}}, -\alpha\sqrt{Dt}\right) \quad (\text{Green's function})$$

$$Q(t | r_0) = \int_R^\infty 4\pi r^2 p(r, t | r_0) dr = 1 + \frac{R\alpha + 1}{r_0\alpha} \left[W\left(\frac{r_0 - R}{\sqrt{4Dt}}, \alpha\sqrt{Dt}\right) - \text{Erfc}\left(\frac{r_0 - R}{\sqrt{4Dt}}\right) \right] \quad (\text{Survival probability})$$

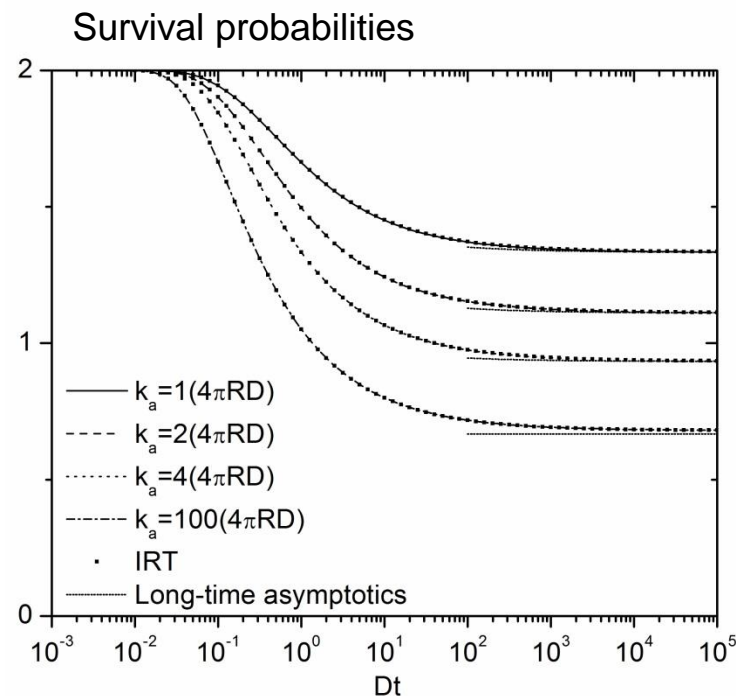
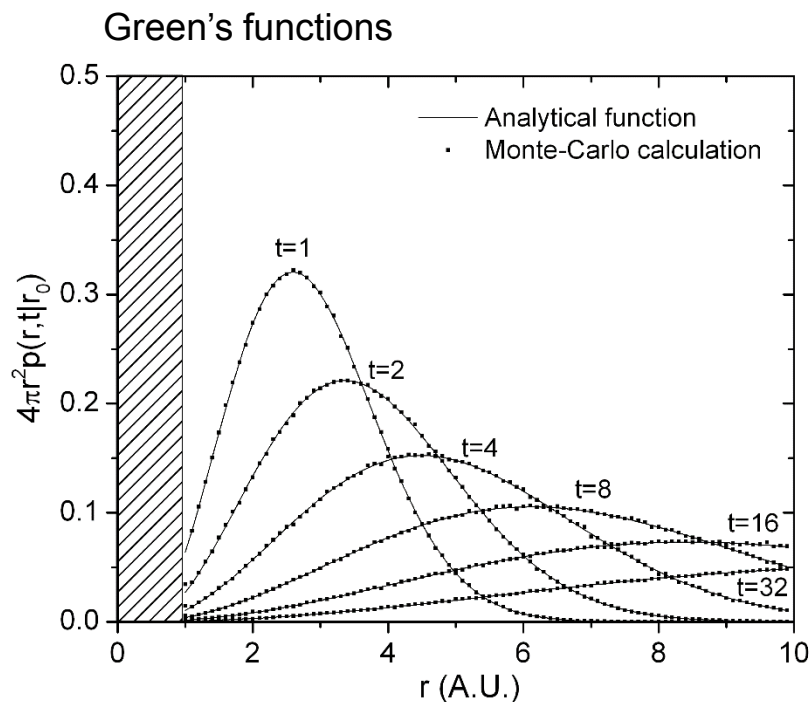
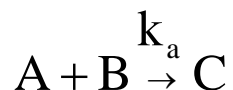
$$\alpha = -\frac{k_a + 4\pi RD}{4\pi R^2 D}$$

The probability of reaction $P(t|r_0) = 1 - Q(t|r_0)$. At each time step, the probability of reaction is assessed. If the particles have not reacted, their relative distance is obtained by sampling the Green's function using the algorithm described in Plante et al. (2013).

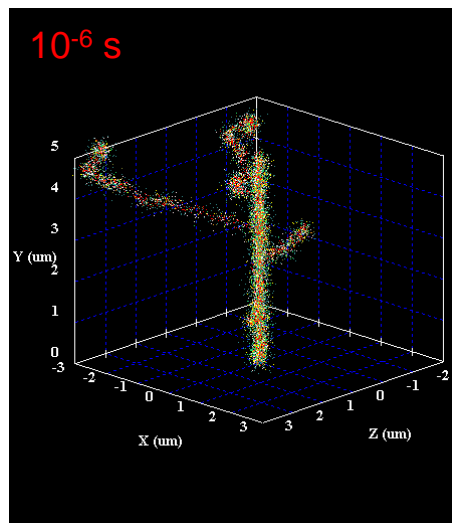
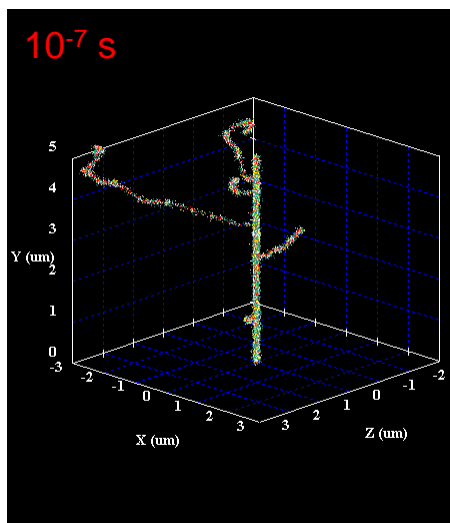
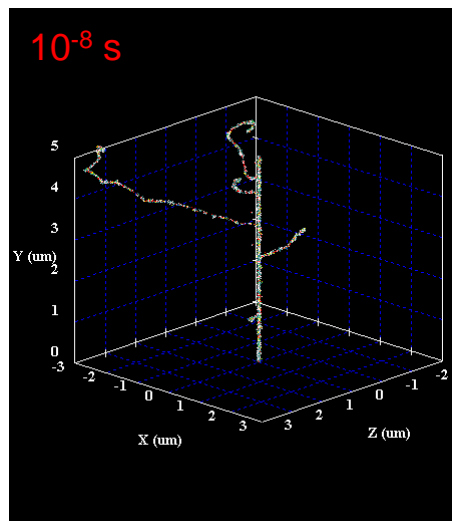
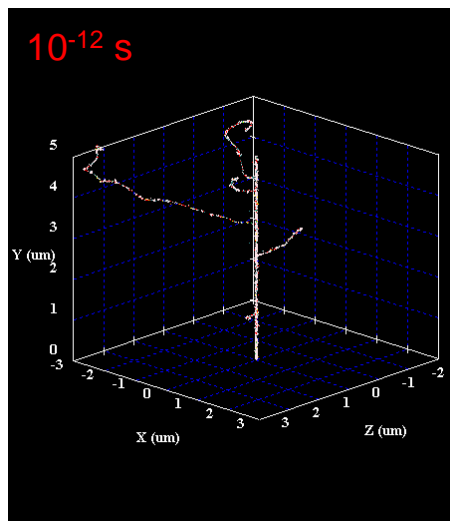
Green's Function for Radiation Chemistry



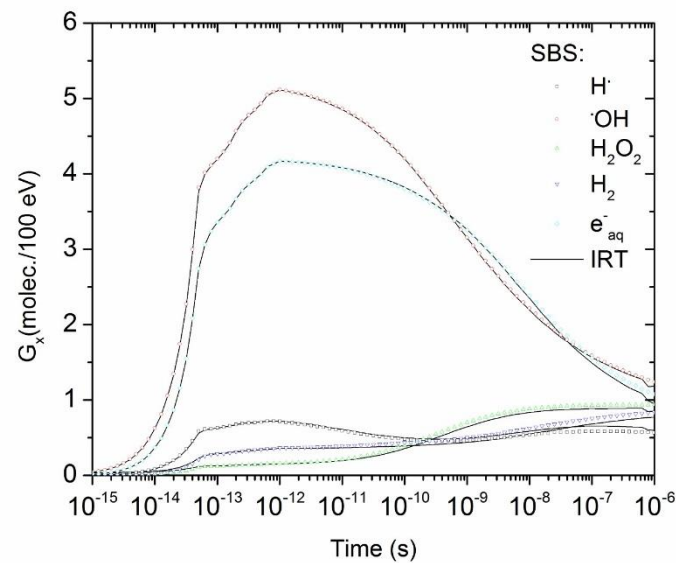
- Simple case: partially diffusion-controlled reaction with rate k_a and reaction radius R



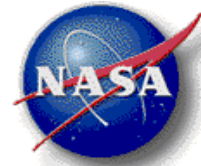
Radiation Chemistry



Simulation of the time evolution of a $^{12}\text{C}^{6+}$ track, 100 MeV/u



Radiation Chemistry

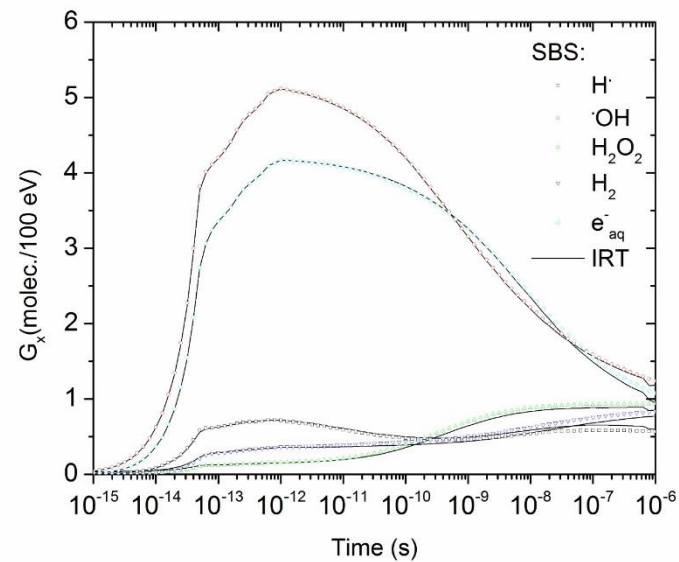
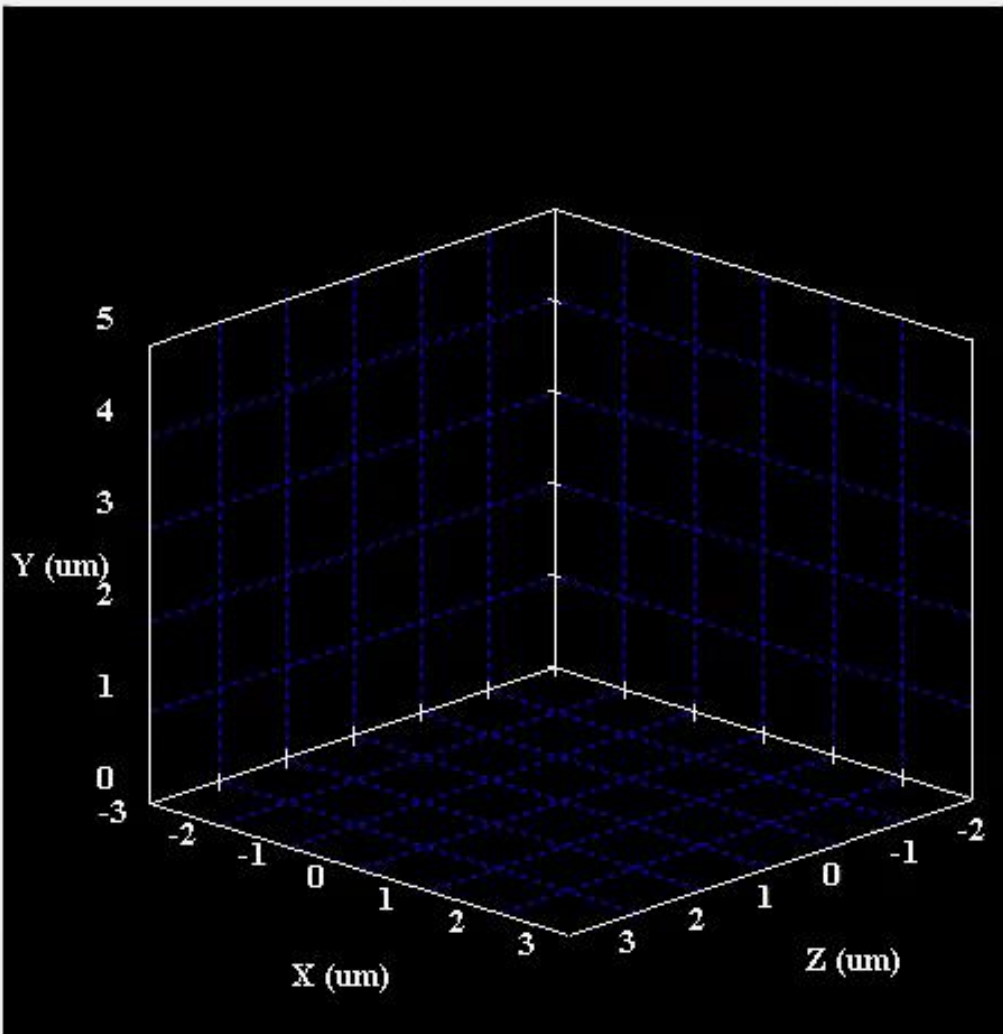


$^{12}_{6}\text{C}^{6+}$

100 MeV/amu

Time: 1.000E-16 s

s

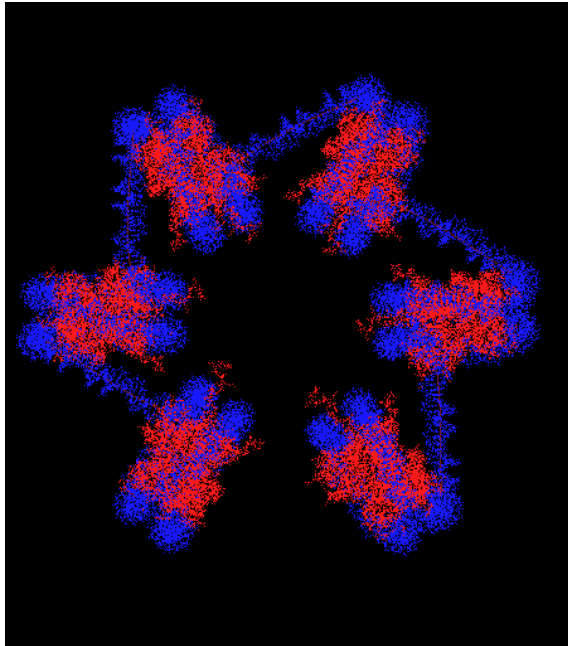


DNA Damage Simulations

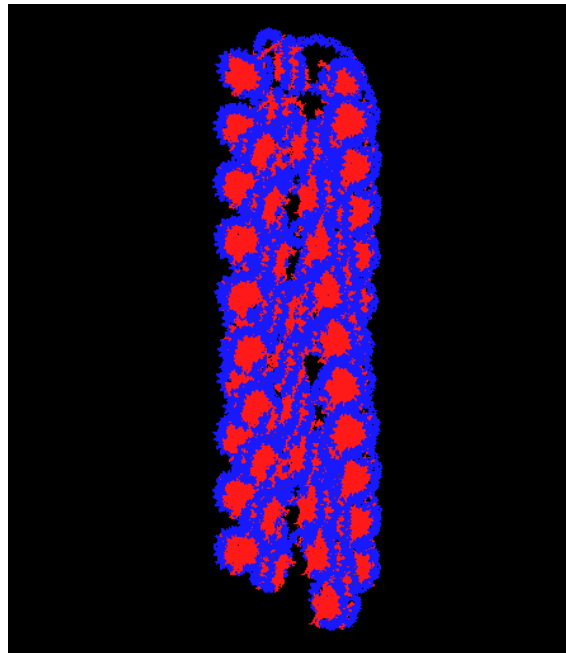


- ❑ To better understand the formation of DSBs, a chromatin fiber is build from nucleosome units and linker DNA

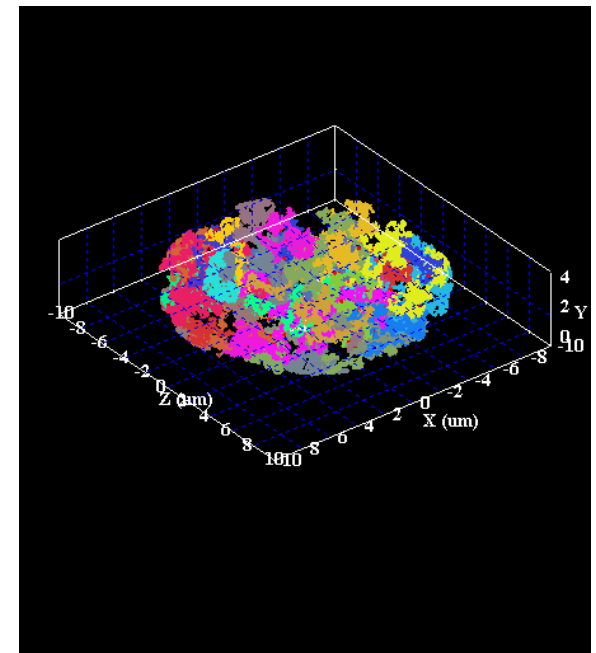
Nucleosome (DNA fragments)



Chromatin fiber



Nuclei



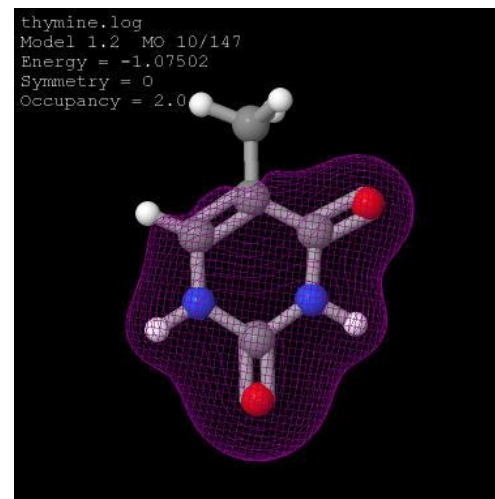
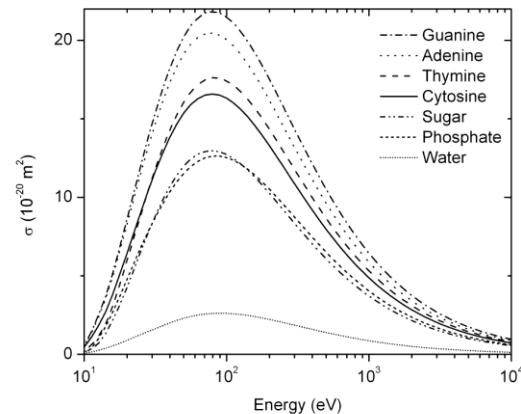
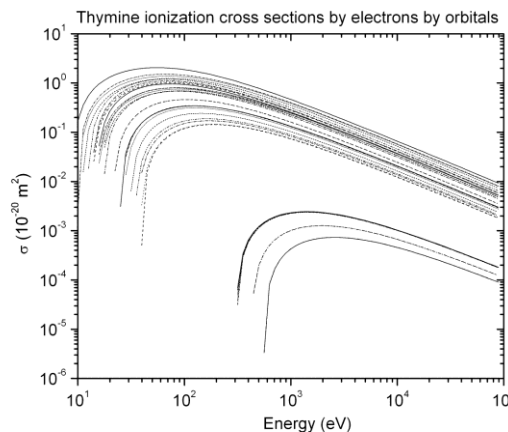
Nuclei simulations courtesy of Artem Ponomarev, PhD

DNA Damage Simulations

- In the DNA bases, there are many internal and valence electrons. The BEB model allows to model the ionization for each electron of the molecule.

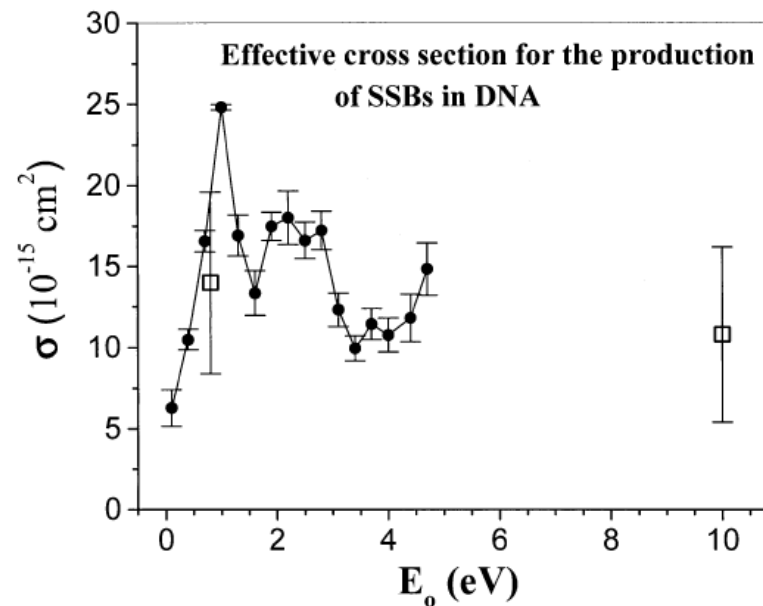
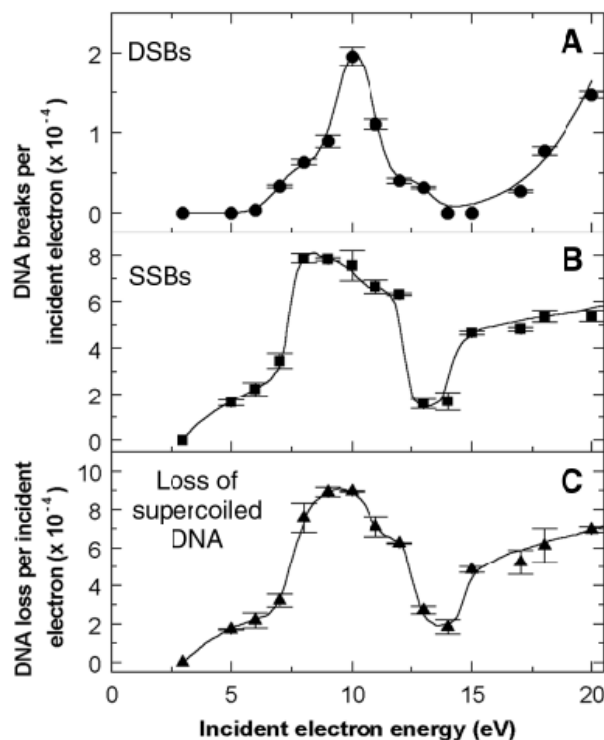
Thymine

	No	U (eV)	B (eV)	N
Internal electrons (18)	1	794.1	559.41	2
	2	794.1	559.18	2
	3	601.5	425.6	2
	4	601.5	425.48	2
	5	435.9	311.36	2
	6	435.9	310.43	2
	7	435.8	308	2
	8	435.7	306.41	2
	9	435.8	305.8	2
Valence electrons (44)	10	66.26	40.06	2
	11	71.74	39.14	2.04
	12	63.05	36.16	1.86
	13	57.89	34.56	1.85
	14	44.95	30	2.3
	15	43.96	26.22	2.35
	16	47.64	25.14	2.11
	17	40.64	24.85	2.15
	18	41.92	21.32	2.18
	19	39.28	20.94	2.02
	20	36.32	19.4	1.86
	21	44.53	18.7	2.05
	22	55.89	18.56	1.92
	23	54.72	17.59	1.99
	24	39.88	16.62	2.01
	25	46.93	16.15	2.03
	26	39.89	15.44	1.78
	27	47.3	13.96	1.83
	28	59.96	13.15	1.86
	29	54.12	12.31	2.07
	30	60.23	12.10	1.78
	31	40.38	9.27	1.97

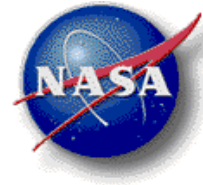


DNA Damage Simulations

- ❑ In addition to ionization, it is now well established that low-energy electrons can damage DNA, including DSB
- ❑ Mechanism: dissociative attachment to resonant states



DNA Damage Simulations

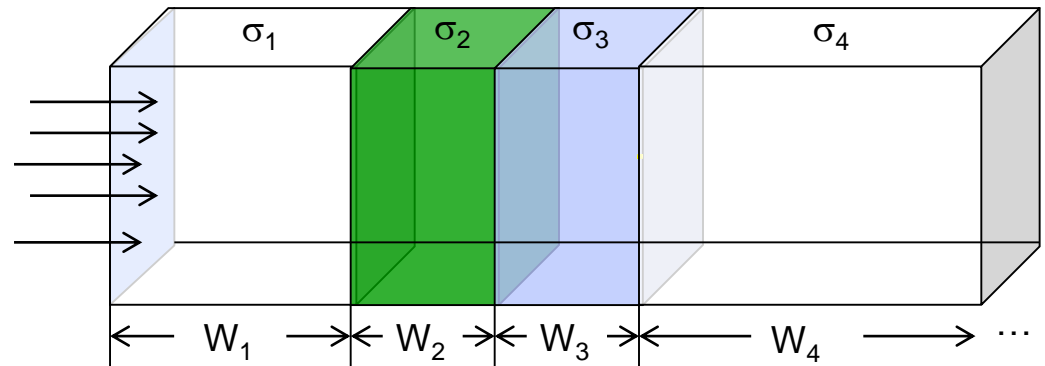


- ❑ Cross sections can be calculated for the bases, sugars and phosphates.
- ❑ In this case, the medium is considered a succession of homogeneous media.

$$dI = -I N \sigma dx$$

$$\ln(I / I_0) = - \int_0^x \sigma(u) N du$$

$$I = I_0 \exp \left\{ -N \left[\sum_{j=1}^{i-1} (\sigma_j - \sigma_i) W_j + \sigma_i x \right] \right\}$$

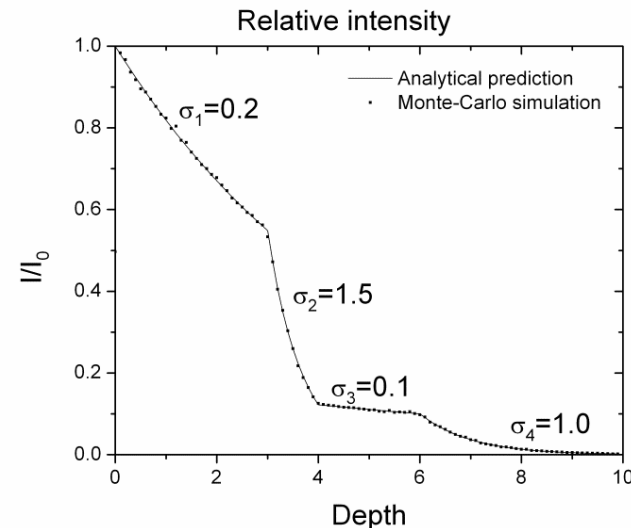


Relative weight

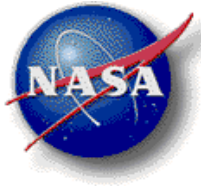
$$p_i = I_0 \frac{\exp(-N \sum_{j=1}^{i-1} W_j \sigma_j) (1 - \exp(-N W_i \sigma_i))}{N \sigma_i}$$

Sampling of W_s

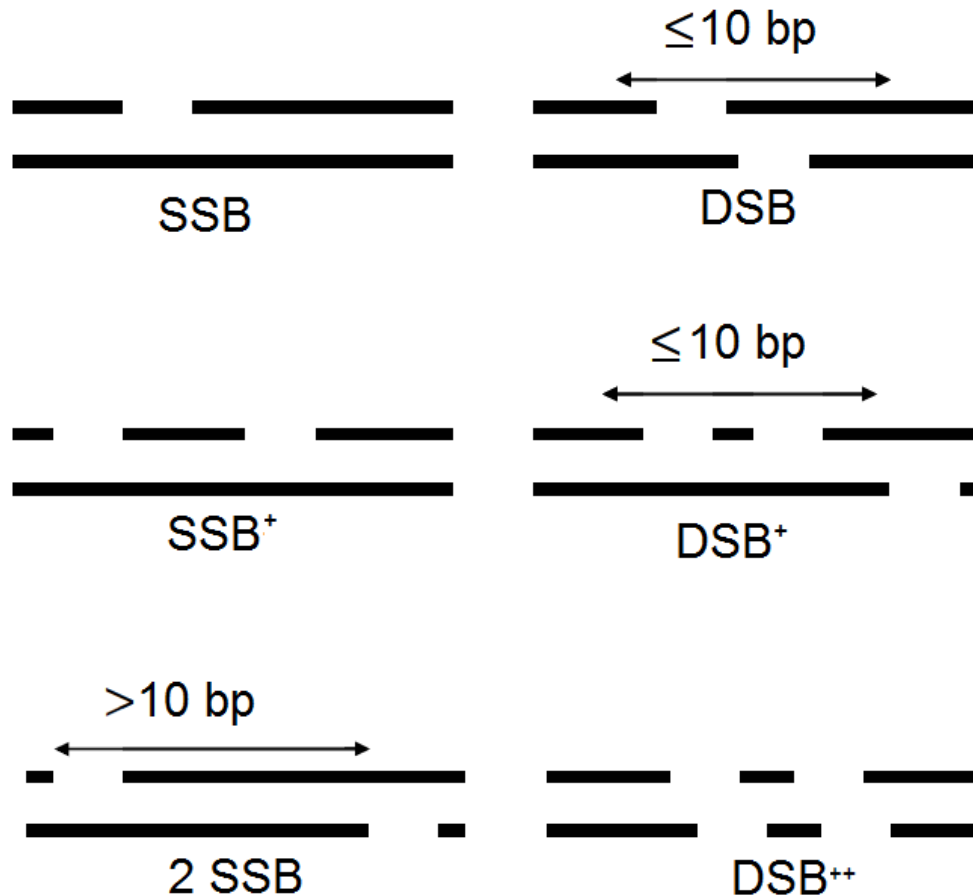
$$W_s = \sum_{j=1}^{i-1} W_j - \frac{1}{N \sigma_i} \log[1 - V(1 - e^{-\sigma_j N W_j})]$$



DNA Damage Simulations



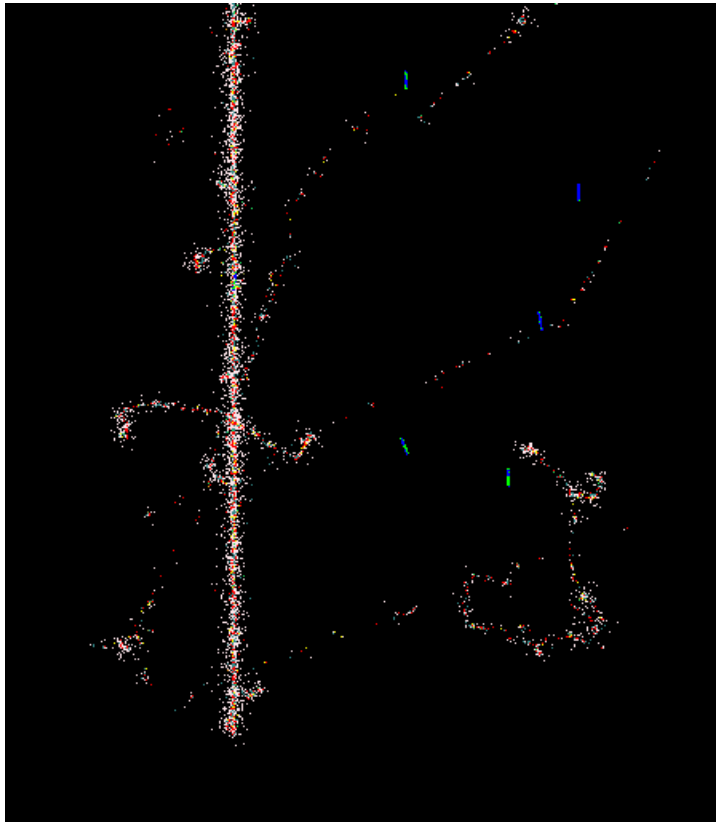
□ Classification of DNA damage



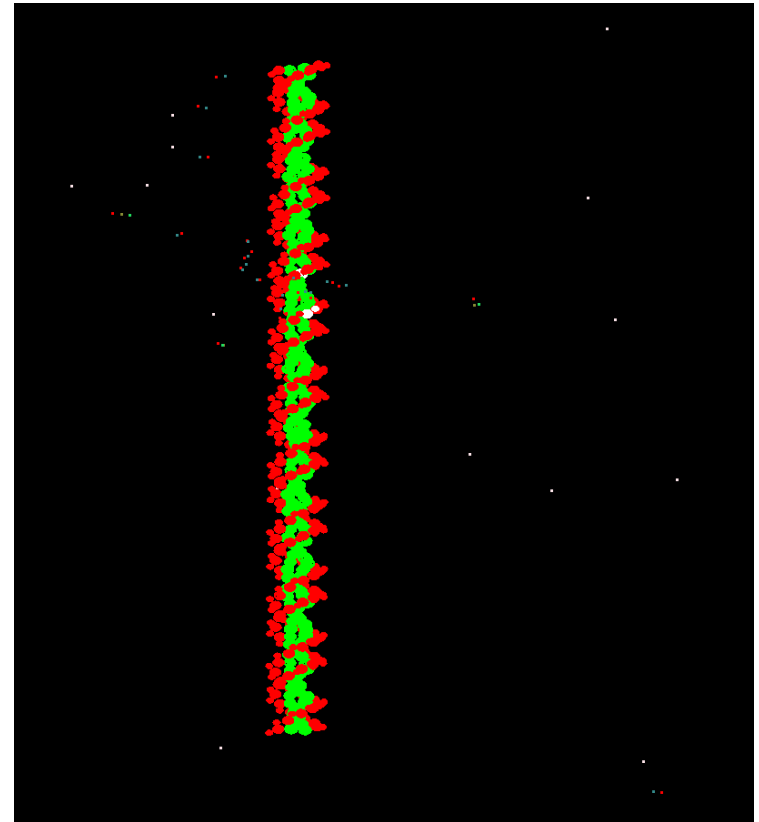
DNA Damage Simulations



❑ Simulation in RITRACKS



DNA fragments in irradiated volume

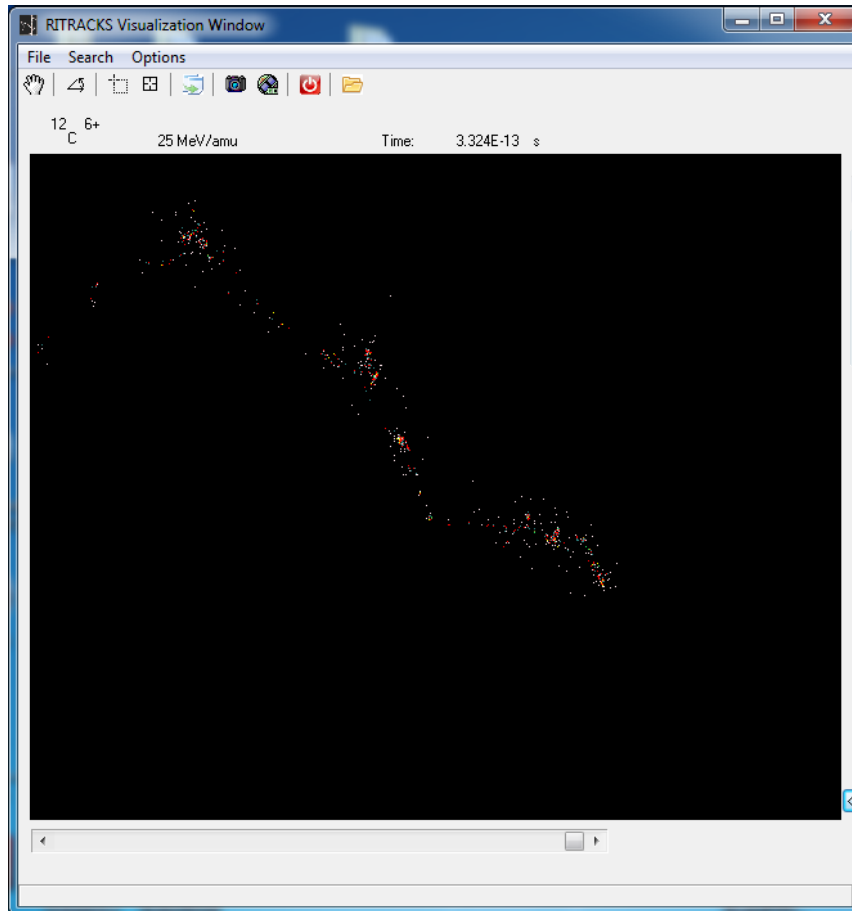


DNA fragment near a track

DNA Damage Simulations



- ❑ Multiple zoom allows better visualization of detailed track-DNA interaction



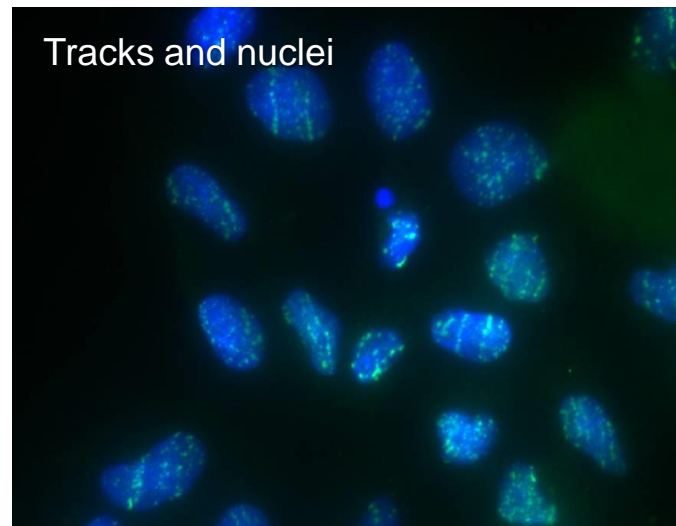
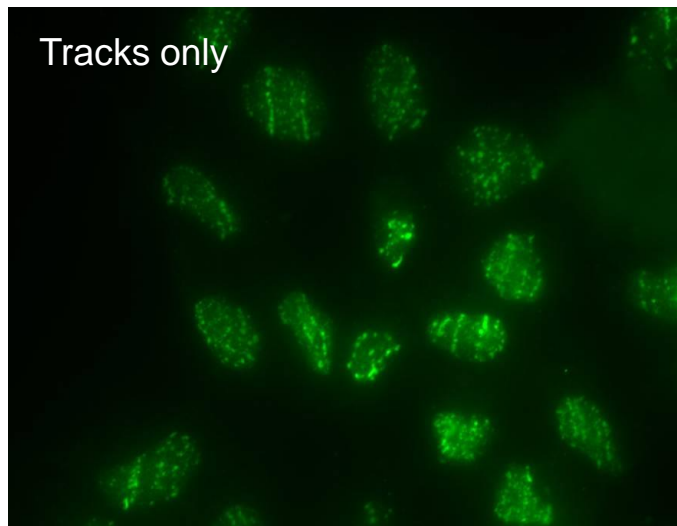
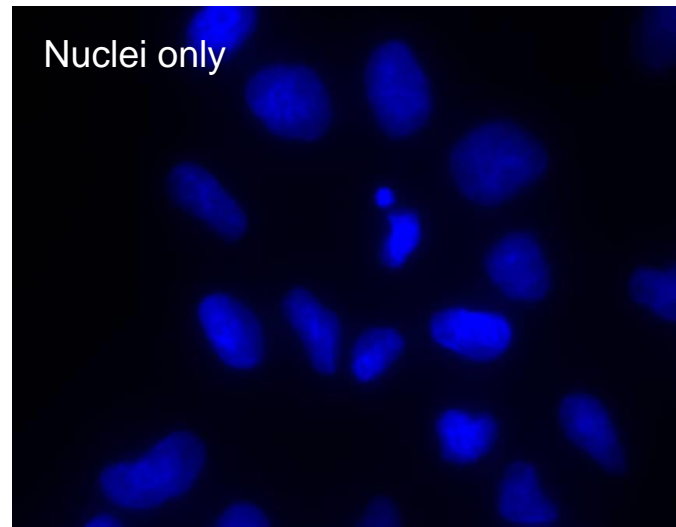
-
- Chemical reaction scheme showing the degradation pathways of 1-methyl-2-pyridone (1) under various conditions:
- Pathway 1:** Reaction with OH^+ (60%) leads to intermediate (2), which reacts with O_2 (diffusion controlled) to form (5), then (8), (14), and finally (11).
 - Pathway 2:** Reaction with OH^- (35%) leads to intermediate (3), which reacts with O_2 (diffusion controlled) to form (6), then (9), and finally (12).
 - Pathway 3:** Reaction with OH^+ (5%) leads to intermediate (4), which reacts with O_2 (diffusion controlled) to form (7), then (10), and finally (15) and (16).

The reaction scheme illustrates the conversion of 4-methyl-2,6-pyridinedione (4) to 4-hydroxymethyl-2,6-pyridinedione (15) and 4-formyl-2,6-pyridinedione (16). The process begins with compound (4), which is oxidized by O_3 (diffusion controlled) to form intermediate (7), 4-(carboxymethyl)-2,6-pyridinedione. Intermediate (7) then undergoes further transformation to form (10), 4-(hydroxymethyl)-2,6-pyridinedione. Finally, (10) is converted into the products (15) and (16).

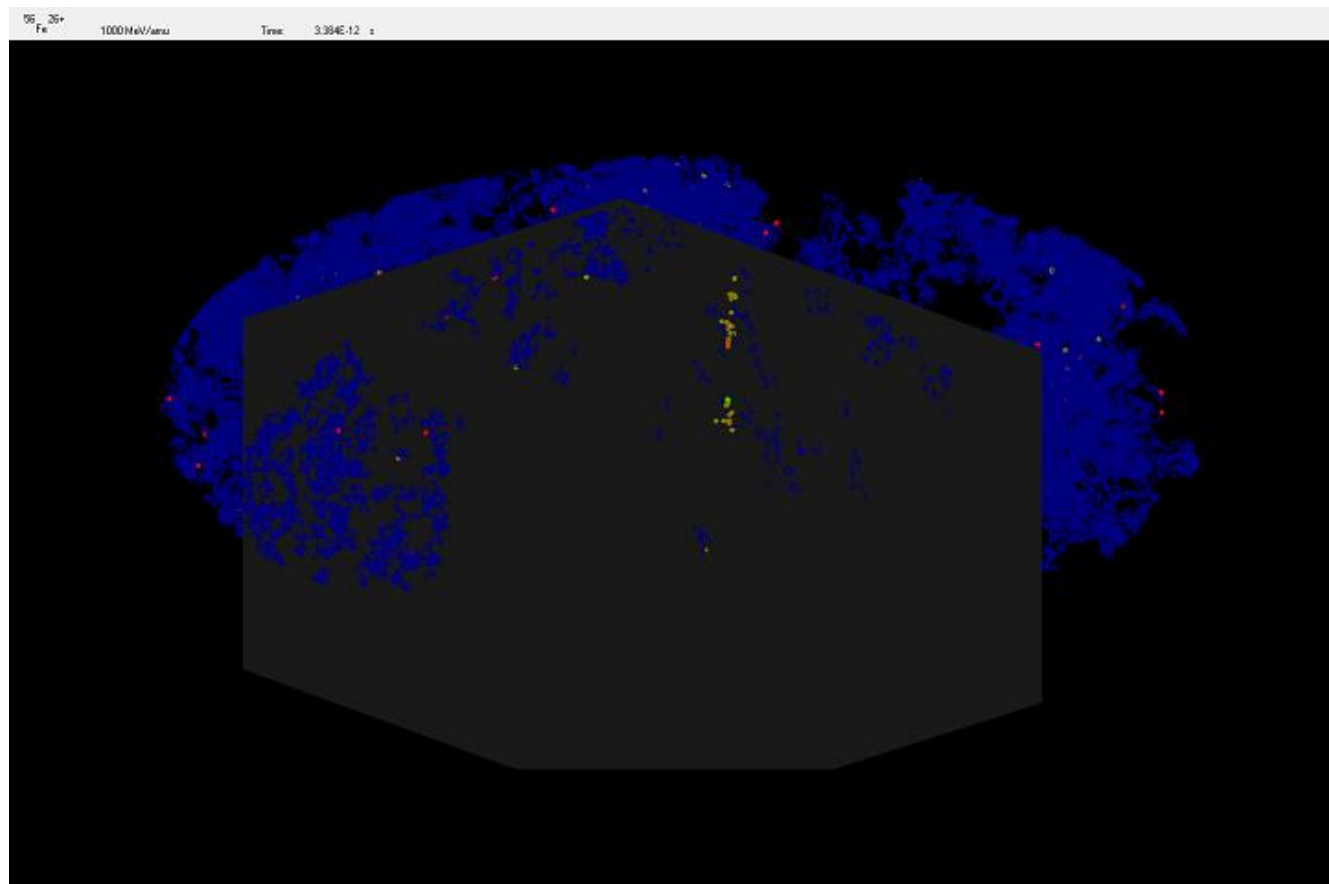
DNA Damage / γ H2AX Foci Studies



- Irradiation by 1 GeV/amu Fe ions
- 100 cGy
- LET ~ 148 keV/ μ m



γ -H2AX Foci Simulations

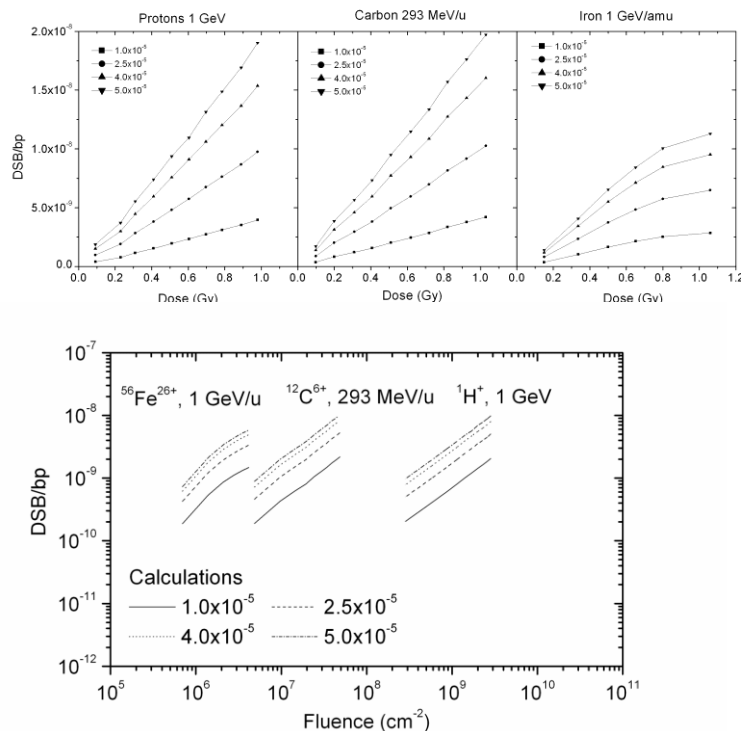


DNA Damage / γ H2AX Foci Studies

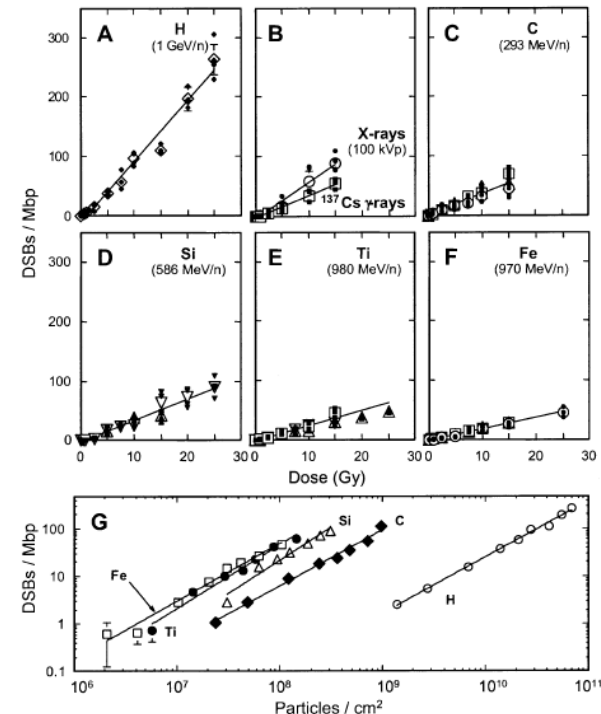


□ Calculation of DSBs by $^1\text{H}^+$, $^{12}\text{C}^{6+}$ and $^{56}\text{Fe}^{26+}$ ions

Simulation results

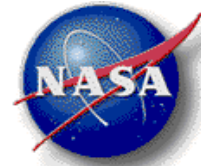


Compare with

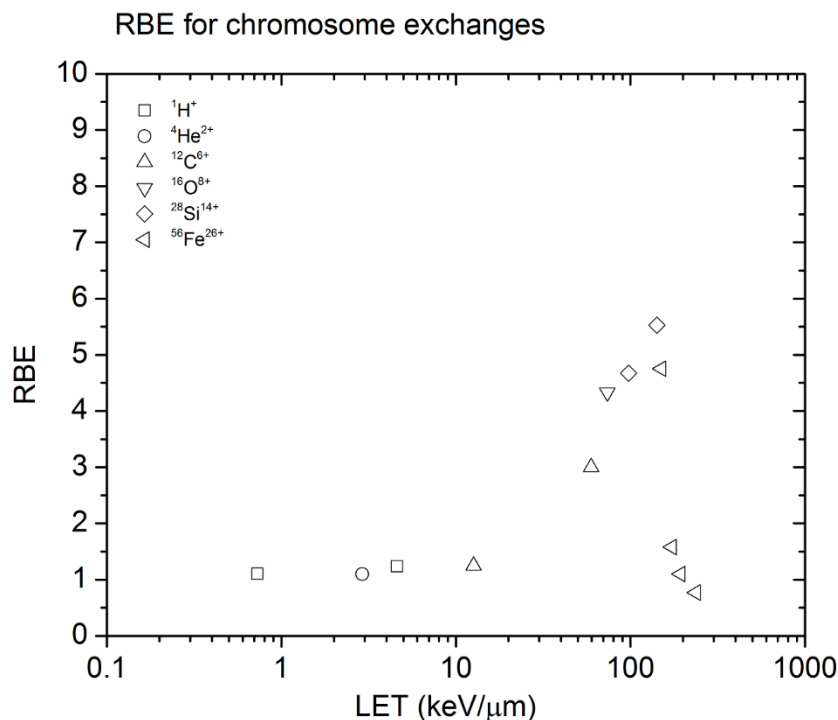
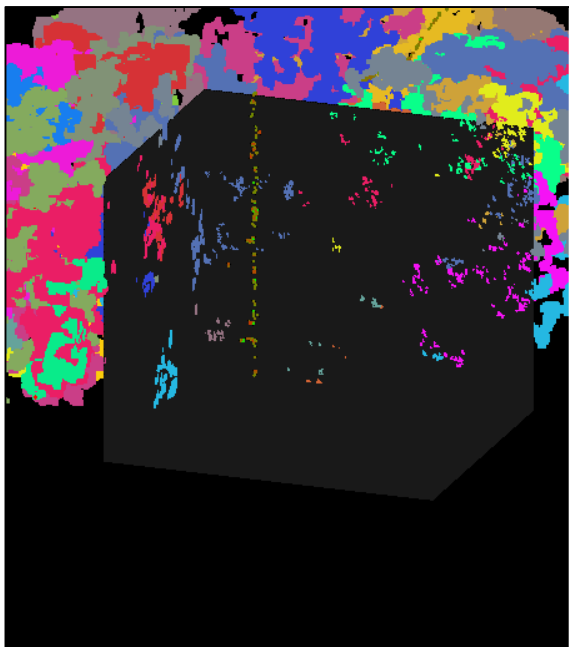


=> Several orders of magnitude of difference but similar trend!

Chromosome Aberrations



- ❑ Damaged DNA may be repaired improperly, leading to various types of chromosome aberrations
- ❑ Chromosome aberrations are linked to cancer and can be used as a biomarker for cancer risk associated with radiation exposure
- ❑ Some ions are more efficient for the creation of chromosome aberrations

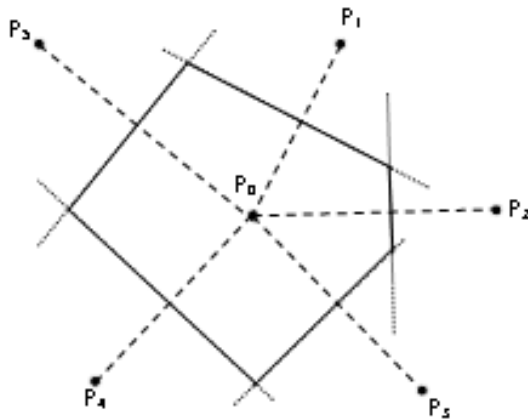


Cells and Tissue Models

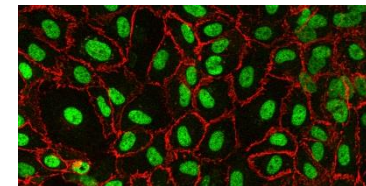
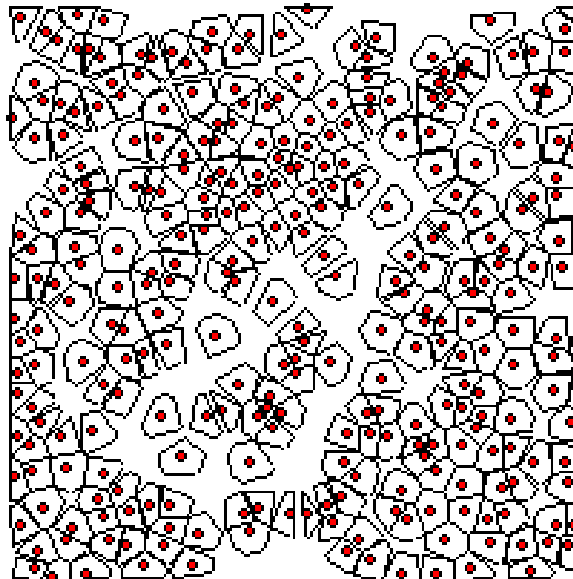


- ❑ Many tissue and cell culture models are based on Voronoi tessellation (in 2D and 3D)
- ❑ A Voronoi cell is the space closest to a given point (than the other points)
- ❑ Models derived from microscopic images can also be used

A 2D voronoi cell



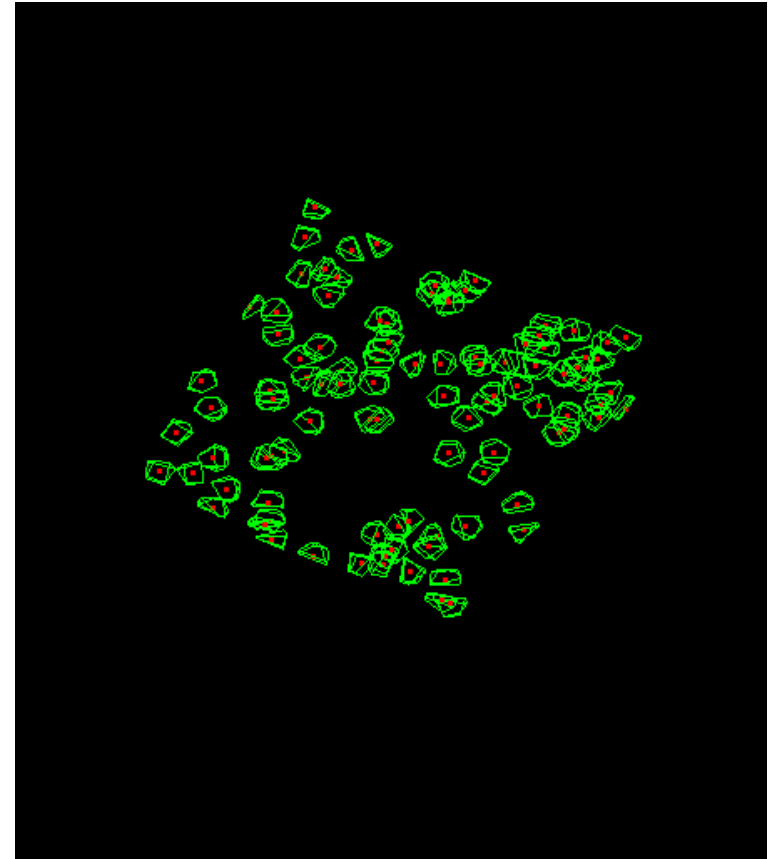
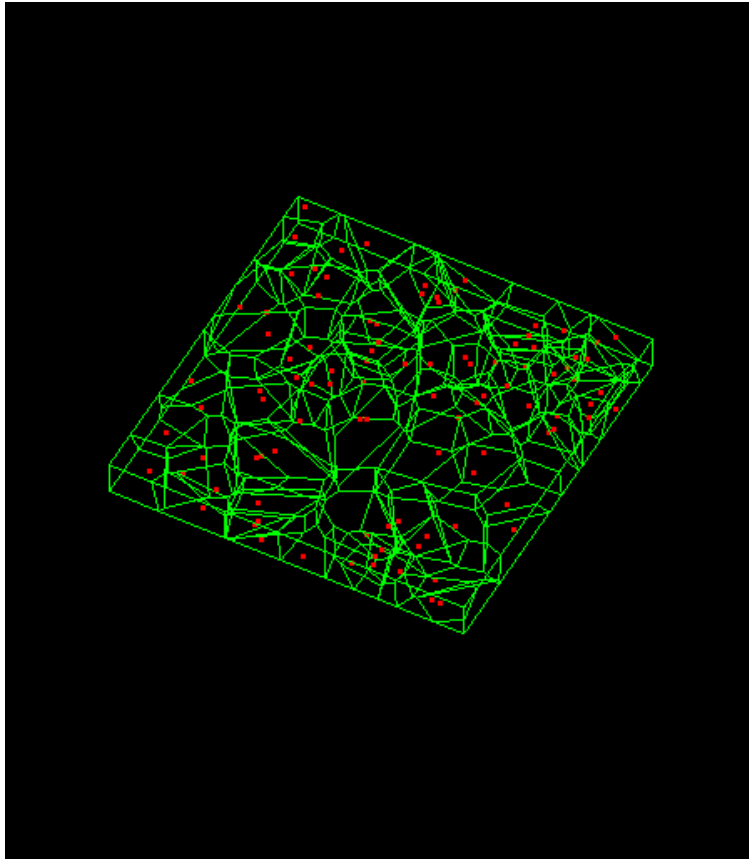
Simulation of a 2D cell culture using a simple Voronoi cell tessellation and clipping



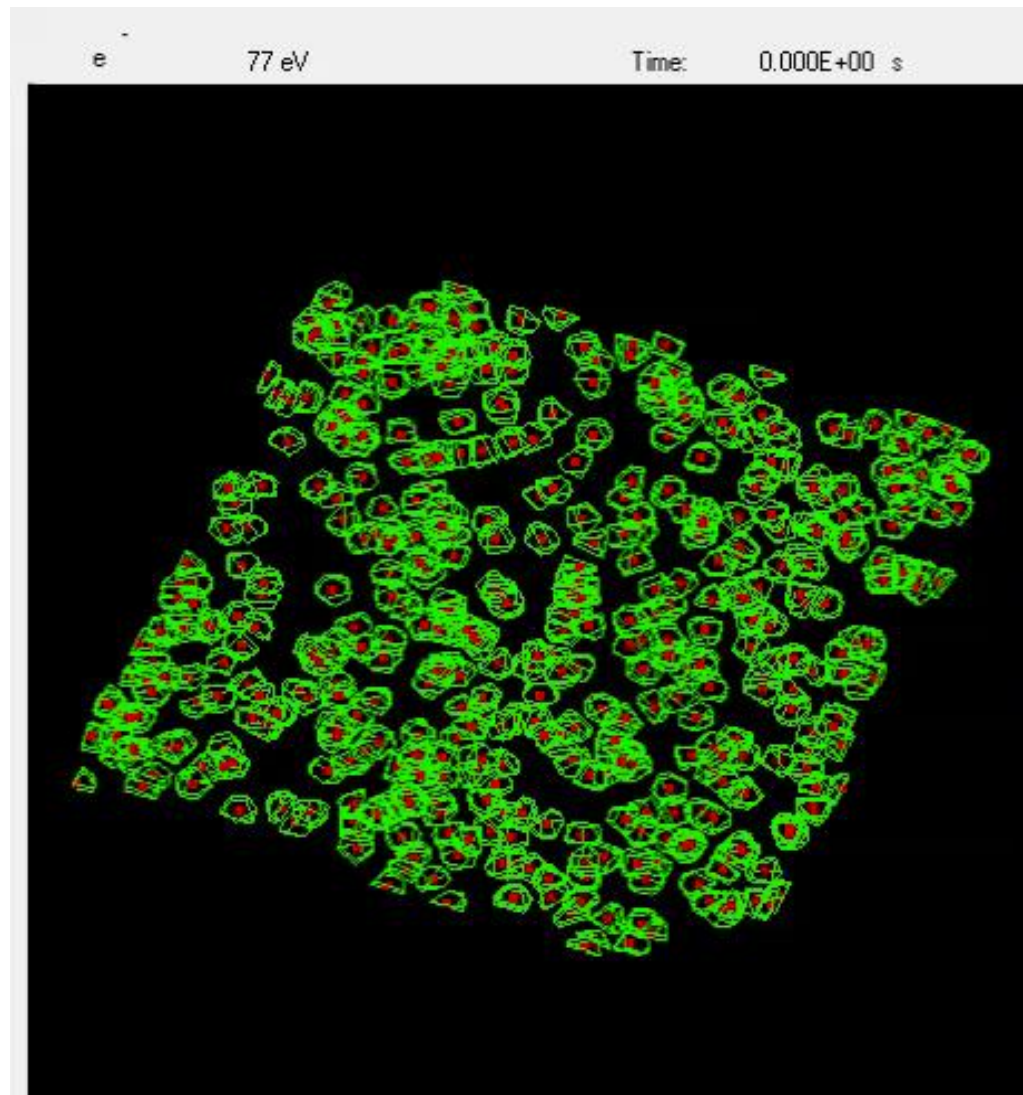
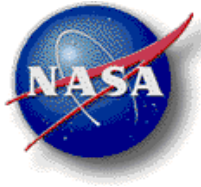
Tissue Models



- ☐ Voronoi cell tessellation in 3D was included in RITRACKS
- ☐ Multi-scale modelling



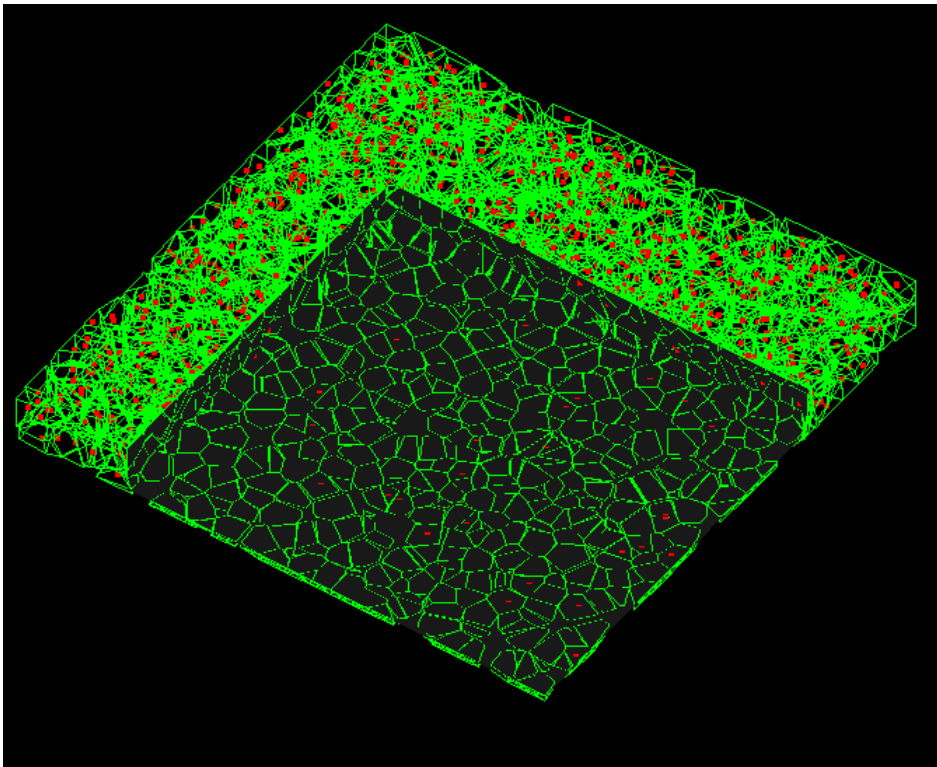
Tissue Models



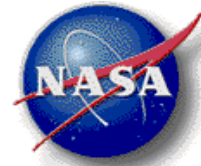
Visualization of 3D Tissue Models



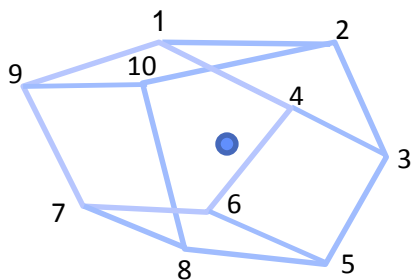
- ❑ In 3D, the space is packed with cells so it is hard to distinguish the cells
- ❑ A visualization tool, the slicer, allows the visualization of planes within the tissue model



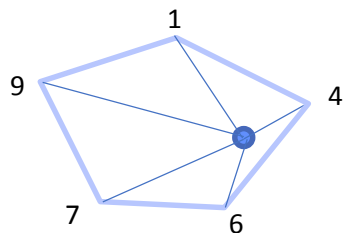
Algorithm to Determine if a Point is Inside a Cell



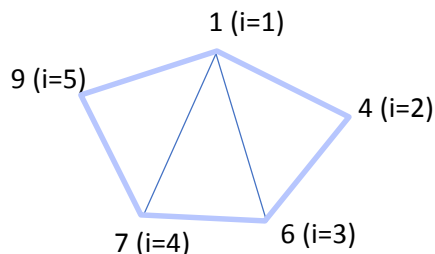
□ Typical Voronoi-like 3D cell



Face	Vertices (in order)
I	1,2,3,4
II	1,9,10,2
III	7,8,10,9
IV	8,7,6,5
V	5,6,4,3
VI	10,8,5,3,2
VII	1,4,6,7,9



Polyhedron face VII



Decomposition of face into triangles

Vertices (1,i+k,i+k+1),
k=1,N-2

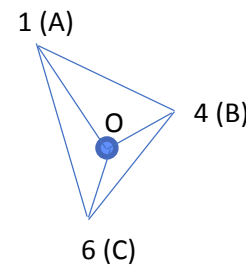
Works for convex figures only!!

Calculation of solid angle (Ω) for each triangle pyramid using L'Huilier's theorem

$$\cos\theta_a = \frac{\overrightarrow{OB} \cdot \overrightarrow{OC}}{\|\overrightarrow{OB}\| \|\overrightarrow{OC}\|}$$

$$\cos\theta_b = \frac{\overrightarrow{OA} \cdot \overrightarrow{OC}}{\|\overrightarrow{OA}\| \|\overrightarrow{OC}\|}$$

$$\cos\theta_c = \frac{\overrightarrow{OA} \cdot \overrightarrow{OB}}{\|\overrightarrow{OA}\| \|\overrightarrow{OB}\|}$$



$$\theta_s = \frac{\theta_a + \theta_b + \theta_c}{2}$$

$$\tan\left(\frac{\Omega}{4}\right) = \sqrt{\tan\left(\frac{\theta_s}{2}\right) \tan\left(\frac{\theta_s - \theta_a}{2}\right) \tan\left(\frac{\theta_s - \theta_b}{2}\right) \tan\left(\frac{\theta_s - \theta_c}{2}\right)}$$

The point is inside the cell if the sum of all solid angles of all triangles of all faces is 4π .

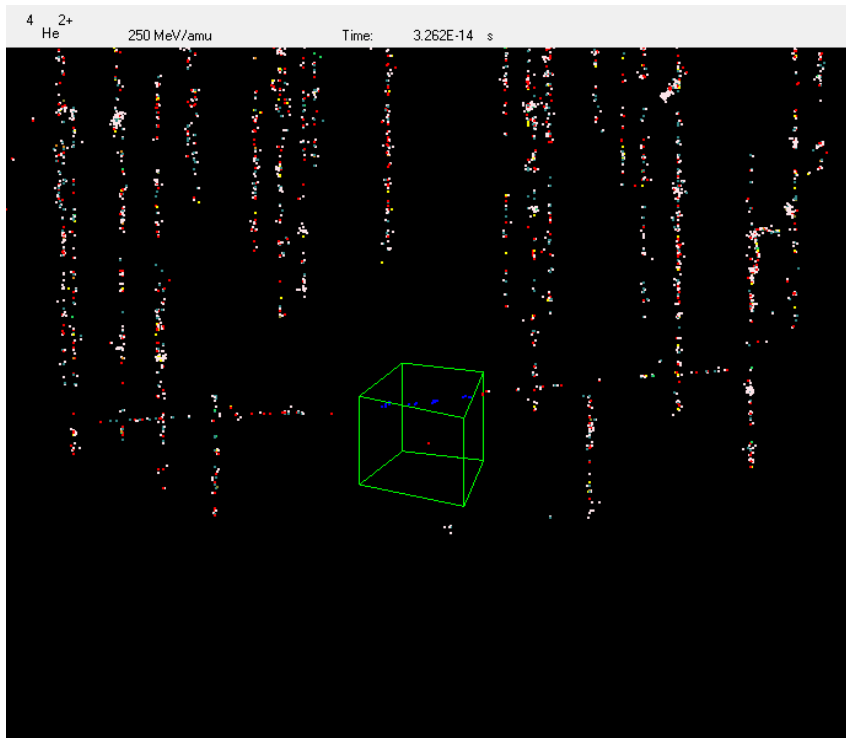
Similarly, the volume of the cell is obtained by summing the volume of all pyramid, using

$$V = \frac{1}{6} \|\overrightarrow{OA} \times \overrightarrow{OB} \cdot \overrightarrow{OC}\|$$

Algorithm to Determine if a Point is Inside a Cell



- ❑ Use with RITRACKS visualization interface
- ❑ The algorithm seems to work fine for the case studied
- ❑ Since the calculation of the volume can be done similarly, dose can be calculated in cells



Comments:

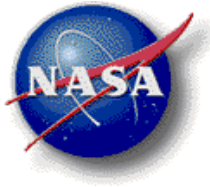
- The algorithm is rather slow. A screening algorithm determine first if the point is inside a sphere encompassing the cell.
- The algorithm is not expected to work for non-convex cells in its actual form.
- The argument inside the square root in L'Huilier's equation is occasionally negative. This problem was solved by taking the absolute value. However it is not clear that doing this is justified and how this affects the algorithm

Future Development Plans



- ☐ Predictions of clustered and complex DNA damage yields in human cells for improving the understanding of DNA repair and signal transduction
- ☐ Use with chromosome models to study double-strand breaks (DSB) and chromosome aberrations in relation to cancer risks from space radiation
- ☐ Links with “Omics” to determine gene and pathways affected by DNA damage and chromosome aberrations
- ☐ Tissue models
- ☐ Web-based version?

Acknowledgements



- ☐ Artem Ponomarev (Wyle)
- ☐ Steve Blattnig (NASA Langley)
- ☐ Shaowen Hu (Wyle)
- ☐ Kerry George (Wyle)
- ☐ Cliff Amberboy (Lockheed Martin)
- ☐ Honglu Wu (NASA JSC)
- ☐ Luc Devroye (McGill University)
- ☐ Arnold Pompos (UT Southwestern)